Hindawi
Advances in Civil Engineering
Volume 2018, Article ID 2060974, 7 pages
https://doi.org/10.1155/2018/2060974

Research Article

Experimental Study on the Mud-Water Inrush Characteristics through Rock Fractures

YanLin Zhao[1,2] **and LianYang Zhang**[3]

[1]*Hunan Provincial Key Laboratory of Safe Mining Techniques of Coal Mines, Work Safety Key Lab on Prevention and Control of Gas and Roof Disasters for Southern Coal Mines, Hunan University of Science and Technology, Xiangtan, Hunan 411201, China*
[2]*State Key Laboratory of Coal Resources and Safety Mining, China University of Mining and Technology, Xuzhou, Jiangsu 221008, China*
[3]*Department of Civil Engineering and Engineering Mechanics, University of Arizona, Tucson, AZ 85721, USA*

Correspondence should be addressed to YanLin Zhao; yanlin_8@163.com

Received 31 August 2017; Accepted 23 April 2018; Published 13 June 2018

Academic Editor: Venu G. M. Annamdas

Fractured rock masses, which are widely distributed in the south of China, have an impartible relationship with mud-water inrush. In order to study the change laws of mud viscosity under different moisture content, flow property, and mechanism of mud-water inrush in fractured rock masses, a NDJ-8S rotary viscometer and a simulation model are used to carry out a series of experimental studies. Tests of mud viscosity show that mud viscosity depends on moisture content, and the relationship between viscosity and moisture content was proposed. Based on mud viscosity results, physical model tests' results indicated that the process of mud-water rush can be divided into four stages: that is, the preparation stage of mud-water mixture burst, the seepage period of mud-water mixture inrush, the nonstable period of mud-water mixture outburst, and the stable period of mud-water mixture outburst. The excavation disturbance, high water pressure, and effect of erosion and corrosion of water were identified as key factors which lead to mud-water inrush in fractured rock masses

1. Introduction

Plenty of underground engineering constructions such as railway tunnel and coal extractions are threatened by various kinds of water inrush and mud gushing in China [1–4]. Research methods of theoretical analysis, laboratory experiments, field investigations, and numerical simulations have always been performed by many scholars and experts to discover the mechanisms and influential factors of water inrush and mud burst in fractured rock masses [5–8]. Accordingly, numerous prevention and treatment technologies were proposed. Physical tests and site investigations of mud-water inrush show that the main factors, related to water-mud burst, are the supply of water, pressure of water, geological structure, engineering excavation, and so on [9–11]. On one hand, the theoretical analysis and numerical simulations also come up with some effective and practical ways to prevent and treat mud-water burst disasters [12–14]. On the other hand, for setting risk countermeasure, eliminating and reducing the adverse influence of risk, many ways of risk evaluation and prediction about mud-water burst in fractured rock masses were raised to disclose potential risk factors [15–18].

In recent years, there have been more than 100 cases of mud-water burst observed in the southwest mountain, especially in Karst areas, such as Yunnan, Guizhou, and Sichuan, causing serious losses of human life and property and deterioration of construction conditions [19–22]. The fractured rock masses in Karst zones as a complex and widespread geological conditions in China, it is extremely easy to induce geologic hazard especially mud-water gushing when the underground engineering goes through it [23–25]. At present, the research on mud-water outburst mechanism is mainly concentrated on reaction of water-rich area, damage of floor strata, and prevention and treatment [26, 27] in addition to some technical solutions for special

Figure 1: Clay soil used in the test.

conditions that depended on different engineering backgrounds. Although many studies on fluid-solid coupling response in coal mass and fractured rock mass have been performed, indicating that the permeability characteristics of coal rock mass are closely related with their mechanical behavior [28–30], the previous studies did not research mud viscosity, pressure of mud-water outburst, and flow laws of mud-water on rock fractures.

Essentially, solid clay cannot flow, only when mixed with water, it can be converted from solid state into fluid state with different viscosity; at the same time, under the pressure of mud-water which exceeds ultimate bearing capacity of rock pillars between Karst zones and tunnel excavation face, mud inrush and water outburst accidents are easily observed. So in this paper, the change laws of mud viscosity under different moisture content have been studied. The study establishes a similar material simulation model called the test device of mud-water burst in confined Karst to experimentally research the flow characteristics of mud on channels under different mud-water pressures. Through laboratory experiments, the process of mud-water outburst in Karst areas was performed many times through which we can deeply understand the comprehension of mud gushing in Karst areas and understand the improving and enriching mechanisms of the mud burst in Karst areas.

2. Tests of Mud Viscosity

2.1. Soil Sample and Experiment Equipment. Selected soil in these tests is widespread in the south of China called red clay; the amount of montmorillonite is 60–65% which is characterized by easily dispersed and high rate of making mud, and the chemical equation of montmorillonite is $(Al_{1.67}Mg_{0.33})[Si_4O_{10}][OH]_2{\cdot}nH_2O$. The major chemical components of red clay are SiO_2, Al_2O_3, Fe_2O_3, CaO, MgO, and so on, and natural moisture content is 6–10%. Firstly, the soil sample is dispersed and exposed to sun for 7 days (Figure 1); during the period of exposure, a wooden stick was used to crush the clay particles successively and then dried under the temperature of 105°C–110°C for 24 h, and the standard soil sieve is used to select three different particle sizes which are 5–10 mm, 2.5~5 mm, and below 2.5 mm. According to the method of earthwork test GB/T50123-1999, using the digital display measurement instrument of

Figure 2: NDJ-8S rotary viscometer.

Table 1: Experimental parameters and design of the soil sample.

Soil sample	Grain composition		
	5–10 mm	2.5~5 mm	2.5~5 mm
Coarse clay	100%	—	—
Medium clay	—	100%	—
Fine clay	—	—	100%
Mixed clay	45%	30%	25%

soil liquid-plastic limit to measure soil moisture content under liquid and plastic limit stages, the measurement results are obtained, and these results show that the moisture content of the plastic limit is 19.8% and liquid limit is 30.2%. The measurement instrument of mud viscosity is the NDJ-8S rotary viscometer as shown in Figure 2.

2.2. Tests' Design and Results Discussion. Three different kinds of particle size clay are divided into four groups: the particle size of 5–10 mm is short for coarse particle clay, 2.5~5 mm is short for medium particle clay, below 2.5 mm is short for fine particle clay and mixed particle size clay. After three mud viscosity experiments on each group were conducted, the mean was calculated. Moreover, the beakers and clay samples of each group were labeled as follows: #1, #2, and #3 for coarse clay; #4, #5, and #6 for medium clay; #7, #8, and #9 for fine clay; and #10, #11, and #12 for mixed clay. According to the national standard GB/T20973-2007, mud viscosity tests were performed. Table 1 shows the experimental parameter and design of the soil sample.

Based on the tests' results (Figure 3), the changes of mud viscosity can be divided into three stages: that is, the mud viscosity declines rapidly at the stage of ab, the decline is slow at the stage of bc, and the decline is kept unchanged at the stage after the point c.

As is shown in Figure 3, when the moisture content is constant, mud viscosity does not vary with particle size, and it means that particle size has little ever no influence on mud viscosity which depends on moisture content completely.

At the stage of ab, the water in the mud is no longer in the form of combined water, but it is in the form of free and

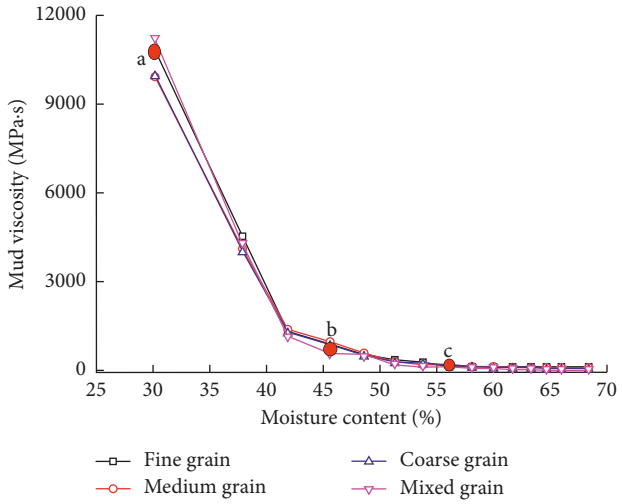

Figure 3: The curves of mud viscosity of different particle sizes under different moisture content.

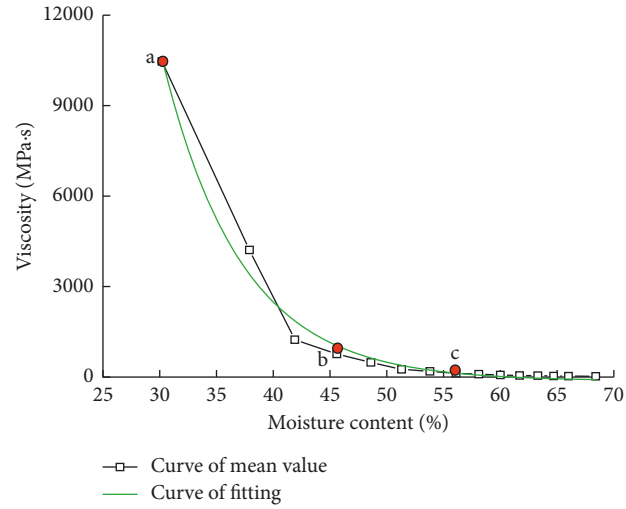

Figure 4: The curve of mud viscosity under different moisture content.

gravity water which can dissolve and erode some soluble bonding material between particles; furthermore, it also has some physical-chemical effects on clay particles, such as lubrication and softening. These poor effects will make the spacing increased between particles, and the chance of interaction reduces, bonding force decreases, and the soil skeleton becomes loose. Meanwhile, at the stage of ab, the viscosity is extremely sensitive to moisture content.

At the stage of bc, mud was in a state of flux completely; moreover, the direction and speed of motion of particles were controlled by water. During the process of mud flow, there is no drag force between particles, but for those which cannot dissolve, during the process of flowing, the sorting phenomenon occurred, which leads to rearrangement and sedimentation of particles and changes mesostructure and mechanical properties of particles. It is the sorting phenomenon caused by water that has large effects on the soil skeleton. But at this stage of bc, mud viscosity is less sensitive to moisture content than the stage of ab.

At the stage after the point c, the viscosity of the mud is tending to be the viscosity of pure water 5.46 MPa·s, and the bonding force and the interaction between the particles in the mud can even be ignored. It is evident that when the moisture content remains the same, the change of viscosity does not vary with the particle size.

The foregoing analysis shows that the mud viscosity does not depend on the particle size but depends on moisture content. Meanwhile, the varying tendencies of each viscosity curve are consistent, no matter how complex the process of the interactions about water and soil is. For further investigation of the relationship between the viscosity and moisture content, the mean method was applied to process each mud viscosity curve of different particle sizes, and then, MATLAB software was used to perform data fitting (Figure 4).

As is shown in Figure 4, at the stage of ab, when the moisture content is below 45%, viscosity will decline rapidly from 10462 MPa·s to 796 MPa·s which is caused by the increase of moisture content in mud; at the stage of bc, when the moisture content is 45%–56%, due to the action of the water, the bonding strength of the mud particle was deteriorative, aerosols were increased, and mud fluidity was enhanced, but with the increase of moisture content in mud, the rate of decline of viscosity slowed significantly; when the moisture content was above 56%, viscosity slowed down extremely as the moisture content of mud increased; finally, change in viscosity remained unchanged (5.46 MPa·s). Mathematical models of the relationship between moisture content and viscosity were obtained by fitting experimental data:

$$v = 8.19 \times 10^5 \exp^{(-(c/6.96))} + 5.52, \quad (1)$$

where c is the moisture content and v is the viscosity.

3. Tests of Mud-Water Inrush

3.1. Equipment and Method. A test device of mud-water inrush through rock fractures was designed to study mud-water inrush characteristics though rock fractures. The skeleton of mud-water inrush through rock fractures is shown in Figure 5, and the test device of mud-water inrush through rock fractures is shown in Figure 6. As shown in Figure 5, the box system in the test device can be divided into three parts: water tank, mud tank, and upper tank, and the size of each part, in turn, is 300 mm × 300 mm × 100 mm, 300 mm × 300 mm × 400 mm, and 300 mm × 300 mm × 800 mm, respectively. The inside of the upper tank was stacked with cement bricks with the size of 70 mm × 70 mm × 70 mm as shown in Figure 7. Mud with a moisture content of 19.8%–30.2% was filled between bricks which were piled up in the upper tank. After mud consolidation, mud and bricks are formed as a whole. The space among the bricks can be considered as rock fractures. The mud tank was used to store mud. In this laboratory mud-water outburst tests, mud with a moisture content of 52% was chosen as mud-water outburst tests' material, and the mud-water

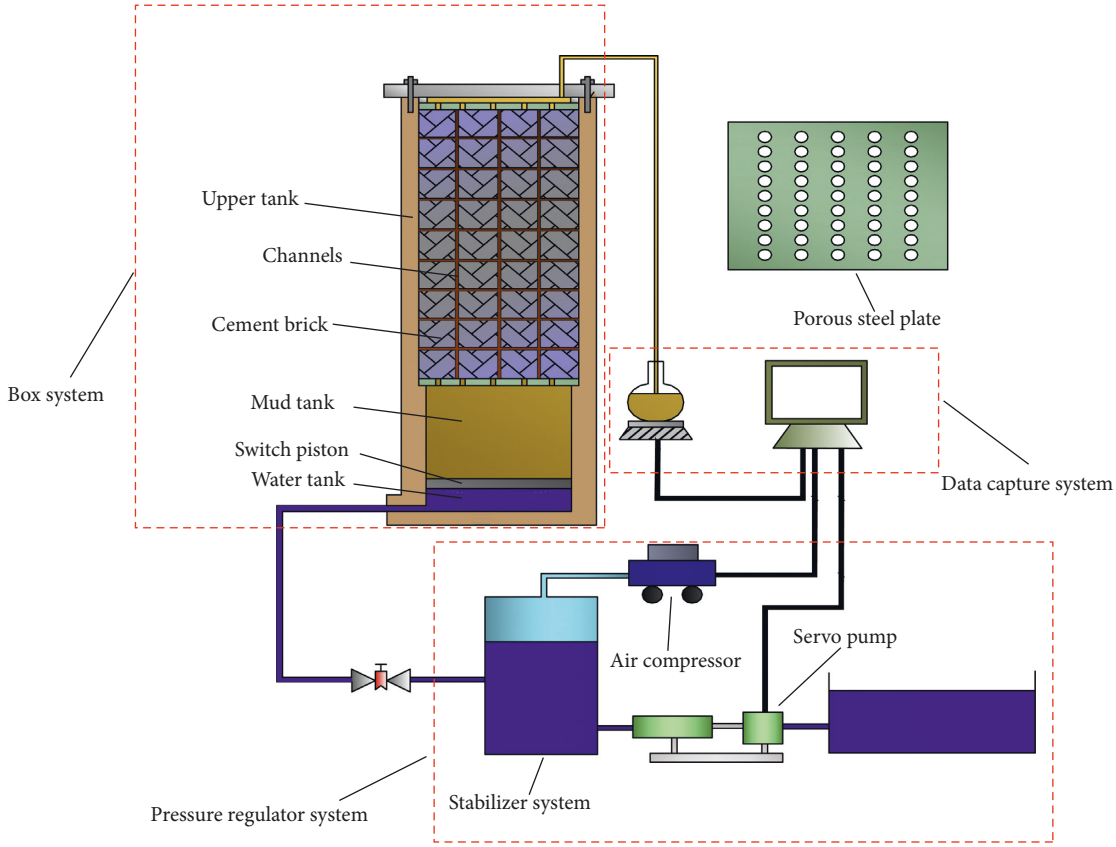

Figure 5: The skeleton of mud-water inrush through rock fractures.

Figure 6: Test device of mud-water inrush through rock fractures.

Figure 7: Cement bricks with the size of 70 mm × 70 mm × 70 mm.

pressure values were set to 0.5, 0.8, 1.0, 1.2, and 1.5 MPa, respectively. At the same time, the mud tank and upper tank are connected through the porous steel plate. On one hand, the porous steel plate can bear the load from all cement bricks which were accumulated in the upper tank; on the other hand, holes in the porous steel plate can allow mud stored in the mud tank to pass through and enter into the upper tank under the water pressure from the water tank. There is a pressure conversion piston between the mud tank and the water tank. The pressure regulator system is made up of an air compressor, a servo pump, and a stabilizer system. During the process of tests, the water pressure in the stabilizer system was monitored in real time by the servo pump; in addition, another important function of the servo pump is to ensure the presence of adequate water in the stabilizer system. If the water pressure in the stabilizer system is below the preset value

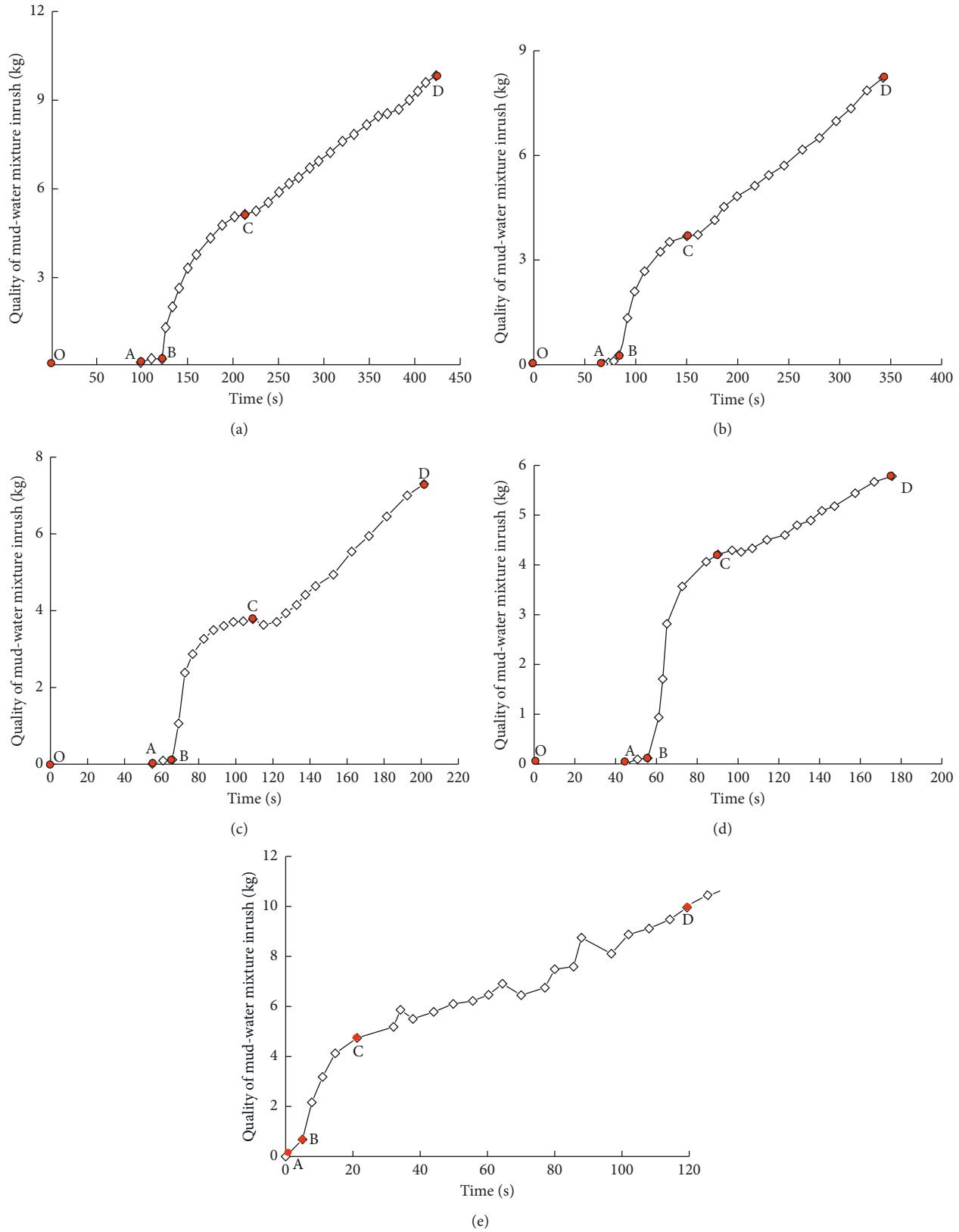

Figure 8: Characteristic curves of mud-water mixture inrush at the mud-water pressures of (a) 0.5, (b) 0.8, (c) 1.0, (d) 1.2, and (e) 1.5 MPa.

which was captured by the servo pump, then the air compressor works, until the water pressure reaches the preset value. According to the field investigation of engineering geological conditions in Karst zones, the mud with a moisture content of 19.8%–30.2% is used as the fillings in the mud tank.

Experimental principles can be summarized as follows: the space among cement bricks (70 mm × 70 mm × 70 mm) to stack each other (11 rows and 4 columns) was regarded as the rock fractures. Meanwhile, the space among bricks was filled with hard plastic clay; cement bricks, which were stacked upon each other, were used to simulate the rock skeleton. After the hard plastic mud was consolidated, the fractured rock mass which was composed of bricks and clay was formed in the upper tank. The fracture widths in the horizontal and vertical directions are about 7 mm and 3 mm, respectively. The water tank is connected to the external stabilizer system; moreover, the pressure and quantity of water in the external stabilizer system were provided by the air compressor and servo pump which were controlled by the computer. Slurry with a moisture content of 52% in the mud tank could pass through the porous steel plate into the top box under water pressure; meanwhile, the physical state of consolidated clay would change from solid to mobile liquid which can flow through the fracture.

3.2. Results and Discussion. Based on the observation and calculation from the physical modeling, the curves of the quality of mud-water mixture and time under different water pressures are obtained (Figure 8 and Table 2).

Based on the test results that were described above (Figure 8), the research results indicate that the changes in the mud-water mixture inrush can be divided into four stages: (1) The preparation stage of mud-water mixture burst (OA curve segment): at this stage, seepage channels of mud-water mixture were not formed, and thus, there was no mud-water mixture collected at the outlet of the test apparatus. Meanwhile, hard plastic clay, which was filled in the fissure, developed into soft-plastic and fluid-plastic states under the effect of washout and erosion of mud-water mixture gradually. This kind of the evolution stage of hard plastic clay from immobility to mobility was named as the preparation stage of mud-water mixture gushing, and the duration time of this phase is T_{OA}. The experiment also revealed that the greater the augment in mud-water pressure, the shorter the duration time of the incubation period. When the pressure increased from 0.5 MPa to 1.2 MPa, the duration of this stage would decrease from 98s to 45 s. But when the mud-water pressure increases to 1.5 MPa, the incubation stage of mud-water mixture outburst fails to be observed, which showed that the hazard of mud-water inrush with the higher pressure has some characteristics of suddenness and violence. (2) The seepage period of mud-water mixture inrush (AB curve segment): mud-water inrush moves in fracture, and the seepage channels of mud-water forms gradually. The seepage velocity is slow, and the duration time of this phase is T_{AB}; moreover, with the increase of mud-water pressure, the duration time of this phase shortens. When the pressure is increased from 0.5 MPa to 1.5 MPa, the duration time of this seepage stage would decrease from 23 s to 5 s. (3) The nonstable period of mud-water mixture outburst (BC curve segment): at this phase, mud-water mixture is continuously scouring channels and gushing forward to external. The velocity of mud-water mixture outburst is constant; in addition, with the increase of mud-water pressure, the energy stored in the mud tank and the maximum velocity of mud-water mixture outburst would be increased. The experiment showed that when the pressure is increased from 0.5 MPa to 1.5 MPa, the maximum velocity of mud-water mixture inrush of this stage would increase from 1.155×10^{-4} $m^3 \cdot s^{-1}$ to $3.380 \times 10^{-4} m^3 \cdot s^{-1}$. (4) The stable period of mud-water mixture outburst (CD curve segment): at this stage, the passages of mud-water inrush form, keeping a near constant velocity of mud-water mixture inrush. This stage lasts for a relatively longer time.

Table 2: Experimental data of mud-water mixture inrush.

Water pressure (MPa)	T_{OA} (s)	T_{AB} (s)	T_{BC} (s)	Maximum mud-water rate ($m^3 \cdot s^{-1}$)
0.5	98	23	128	1.155×10^{-4}
0.8	69	15	67	0.804×10^{-4}
1	55	10	44	2.090×10^{-4}
1.2	45	9	46	2.953×10^{-4}
1.5	0	5	16	3.380×10^{-4}

4. Conclusions

This paper conducted a series of mud viscosity experiments and chose mud-water with a moisture content of 52% as the tests' material. The process of mud-water in rock fractures was simulated. The research results can be drawn as follows:

(1) The mud viscosity does not depend on the particle size but depends on moisture content. Moreover, the relationship between moisture content and viscosity can be represented by the exponential function.

(2) The process of mud-water inrush can be divided into four stages: that is, the preparation stage of mud-water mixture burst, the seepage period of mud-water mixture inrush, the nonstable period of mud-water mixture outburst, and the stable period of mud-water mixture outburst.

(3) The duration time of the preparation stage and seepage period is shorter, and the maximum velocity of mud-water mixture inrush is larger with the increase in mud-water pressure.

Conflicts of Interest

The authors declare that they have no conflicts of interest.

Acknowledgments

This research is supported by the National Natural Science Foundation of China (nos. 51774131, 51274097, and 51434006), the CRSRI Open Research Program (CKWV2017508/KY), and the Open Projects of State Key Laboratory of Coal Resources and Safe Mining, CUMT (no. SKLCRSM16KF12).

References

[1] J. A. Wang and H. D. Park, "Coal mining above a confined aquifer," *International Journal of Rock Mechanics and Mining Sciences*, vol. 40, no. 4, pp. 537–551, 2003.

[2] Q. Wu, M. Y. Wang, and X. Wu, "Investigations of groundwater bursting into coal mine seam floors from fault zones," *International Journal of Rock Mechanics and Mining Sciences*, vol. 41, no. 4, pp. 557–571, 2004.

[3] Y. Zhao, P. F. Li, and S. M. Tian, "Prevention and treatment technologies of railway tunnel water inrush and mud gushing in china," *Journal of Rock Mechanics and Geotechnical Engineering*, vol. 5, no. 6, pp. 468–477, 2013.

[4] R. Zhang, Z. Q. Jiang, H. Y. Zhou, C. W. Yang, and S.J. Xiao, "Groundwater outbursts from faults above a confined aquifer in the coal mining," *Natural Hazards*, vol. 71, no. 3, pp. 1861–1872, 2014.

[5] H. Wang, H. Lin, and P. Cao, "Correlation of UCS rating with Schmidt hammer surface hardness for rock mass classification," *Rock Mechanics and Rock Engineering*, vol. 50, no. 1, pp. 195–203, 2017.

[6] H. Lin, W. Xiong, and Q. X. Yan, "Three-dimensional effect of tensile strength in the standard Brazilian test considering contact length," *Geotechnical Testing Journal*, vol. 39, no. 1, pp. 137–143, 2016.

[7] Y. L. Zhao, Y. X. Wang, W. J. Wang, W. Wan, and J. Z. Tang, "Modeling of non-linear rheological behavior of hard rock using triaxial rheological experiment," *International Journal of Rock Mechanics and Mining Sciences*, vol. 93, pp. 66–75, 2017.

[8] Q. Wu, Y. Z. Liu, L. H. Luo, S. Q. Liu, W. J. Sun, and Y. F. Zeng, "Quantitative evaluation and prediction of water inrush vulnerability from aquifers over-lying coal seams in Donghuantuo Coal Mine, China," *Environmental Earth Sciences*, vol. 74, no. 2, pp. 1492–1437, 2015.

[9] Y. L. Zhao, L. Y. Zhang, W. J. Wang, W. Wan, and W. H. Ma, "Separation of elasto-visco-plastic strains of rock and a nonlinear creep model," *International Journal of Geomechanics*, vol. 18, no. 1, 2018.

[10] S. C. Li, R. T. Liu, and Q. S. Zhang, "Protection against water or mud inrush in tunnels by grouting: a review," *Journal of Rock Mechanics and Geotechnical Engineering*, vol. 8, no. 5, pp. 753–766, 2016.

[11] G. H. Zhang, L. Song, and L. B. Chen, "A case study on treatment measures for a rock tunnel with inrush mud and sand gushing disaster," *Disaster Advances*, vol. 5, no. 4, pp. 489–493, 2012.

[12] H. H. Wei, "Prevention and treatment measures of water inrush and mud outburst in Xiamen Xiang'an subsea tunnel," *Construction Technology*, vol. 12, pp. 12–15, 2015.

[13] W. Yu, *On Treatment Measures of Water Inrush and Burst Mud at Rock Tunnels*, Shanxi Architecture, Shanxi, China, 2015.

[14] Y. L. Zhao, L. Y. Zhang, W. J. Wang, C. Z. Pu, W. Wan, and J. Z. Tang, "Cracking and stress–strain behavior of rock-like material containing two flaws under uniaxial compression," *Rock Mechanics and Rock Engineering*, vol. 49, pp. 2665–2687, 2016.

[15] J. H. Hwang and C. C. Lu, "A semi-analytical method for analyzing the tunnel water inflow," *Tunnelling and Underground Space Technology*, vol. 22, no. 1, pp. 39–46, 2007.

[16] M. M. Fouladgar, A. Yazdani-Chamzini, and E. K. Zavadskas, "Risk evaluation of tunneling projects," *Archives of Civil and Mechanical Engineering*, vol. 12, no. 1, pp. 1–12, 2012.

[17] J. Curiel-Esparza and J. Canto-Perello, "Selecting utilities placement techniques in urban underground engineering," *Archives of Civil and Mechanical Engineering*, vol. 13, no. 2, pp. 276–285, 2013.

[18] J. Canto-Perello, J. Curiel-Esparza, and V. Calvo, "Criticality and threat analysis on utility tunnels for planning security policies of utilities in urban underground space," *Expert Systems with Applications*, vol. 40, no. 11, pp. 4707–4714, 2013.

[19] Y. H. Ge, *Study on Water Inrush Risk and Early Warning Mechanism of Karst Tunnel*, Shangdong University, Jinan, China, 2010.

[20] J. W. Zhou, "Coping with mud/water bursting in tunnel construction: case study on Baiyun tunnel," *Tunnel Construction*, vol. 31, no. 4, pp. 504–509, 2011.

[21] Y. L. Zhao, L. Y. Zhang, W. J. Wang et al., "Creep behavior of intact and cracked limestone under multi-level loading and unloading cycles," *Rock Mechanics and Rock Engineering*, vol. 50, no. 6, pp. 1–16, 2017.

[22] L. C. Li, T. H. Yang, Z. Z. Liang, W. C. Zhu, and C. A. Tang, "Numerical investigation of groundwater outbursts near faults in underground coal mines," *International Journal of Coal Geology*, vol. 85, no. 3-4, pp. 276–288, 2011.

[23] Y. L. Zhao, S. L. Luo, and Y. X. Wang, "Numerical analysis of Karst cave water inrush and a criterion for the setting width of water-resistant rock pillar," *Mine Water and Environment*, vol. 36, no. 4, pp. 508–519, 2017.

[24] Y. L. Zhao, L. Y. Zhang, W. J. Wang, J. Z. Tang, H. Lin, and W. Wan, "Transient pulse test and morphological analysis of single rock fractures," *International Journal of Rock Mechanics and Mining Sciences*, vol. 91, pp. 139–154, 2017.

[25] M. Babiker and A. Gudmundsson, "The effects of dykes and faults on groundwater flow in an arid land: the red sea hills, Sudan," *Journal of Hydrology*, vol. 297, no. 1, pp. 256–273, 2004.

[26] J. S. Caine, J. P. Evans, and C. B. Forster, "Fault zone architecture and permeability structure," *Geology*, vol. 24, no. 11, pp. 1025–1028, 1996.

[27] W. C. Zhu and C. H. Wei, "Numerical simulation on mining-induced water inrushes related to geologic structures using a damage-based hydro mechanical model," *Environmental Earth Sciences*, vol. 62, no. 1, pp. 43–54, 2011.

[28] Y. S. Zhao, Y. Q. Hu, J. P. Wei, and D. Yang, "The experimental approach to effective stress law of coal mass by effect of methane," *Transport in Porous Media*, vol. 53, pp. 235–244, 2003.

[29] Y. S. Zhao, Z. J. Feng, Z. C. Feng, D. Yang, and W. G. Liang, "THM (Thermo-hydro-mechanical) coupled mathematical model of fractured media and numerical simulation of a 3D enhanced geothermal system at 573 K and buried depth 6000-7000 M," *Energy*, vol. 82, pp. 193–205, 2015.

[30] Y. L. Zhao, J. Z. Tang, Y. Chen, L. Y. Zhang, W. J. Wang, and J. P. Liao, "Hydromechanical coupling tests for mechanical and permeability characteristics of fractured limestone in complete stress–strain process," *Environmental Earth Sciences*, vol. 76, no. 1, pp. 1–18, 2017.